



---

## Slow Movements of Bio-Inspired Limbs

Sarine Babikian<sup>1,3</sup> · Francisco J. Valero-Cuevas<sup>1,2</sup> ·  
Eva Kanso<sup>3</sup>

Received: 14 October 2015 / Accepted: 15 April 2016  
© Springer Science+Business Media New York 2016

**Abstract** Slow and accurate finger and limb movements are essential to daily activities, but the underlying mechanics is relatively unexplored. Here, we develop a mathematical framework to examine slow movements of tendon-driven limbs that are produced by modulating the tendons' stiffness parameters. Slow limb movements are *driftless* in the sense that movement stops when actuations stop. We demonstrate, in the context of a planar tendon-driven system representing a finger, that the control of stiffness suffices to produce stable and accurate limb postures and quasi-static (slow) transitions among them. We prove, however, that stable postures are achievable only when tendons are pretensioned, i.e., they cannot become slack. Our results further indicate that a non-smoothness in slow movements arises because the precision with which individual stiffnesses need to be altered changes substantially throughout the limb's motion.

**Keywords** Biomechanics · Slow limb movements · Driftless systems

**Mathematics Subject Classification** 92B05 · 70E55 · 70Q05 · 70E60

---

Communicated by Paul K. Newton.

---

Valero-Cuevas and Kanso have equal leadership of this paper.

---

✉ Eva Kanso  
kanso@usc.edu

<sup>1</sup> Biomedical Engineering, University of Southern California, Los Angeles, CA, USA

<sup>2</sup> Biokinesiology and Physical Therapy, University of Southern California, Los Angeles, CA, USA

<sup>3</sup> Aerospace and Mechanical Engineering, University of Southern California, Los Angeles, CA, USA

## 1 Introduction

Bio-inspired tendon-driven limbs are widely utilized in the development of several robotics devices, from robot hands and arms, to end effectors for surgical robots (Lee et al. 1994; Jung et al. 2007; Frecker and Snyder 2005; Simaan et al. 2009). Many of these mechanisms employ an actuation based on the length change of elastic—spring-like—tendons, e.g., by using motors that behave like linear springs to generate movement. Changing the stretched length of elastic tendons generates a force that in turn creates a torque at the joints. The same force may be produced by changing the spring constant, or stiffness, of the tendon. Here we propose a computational framework for slow movements of tendon-driven limbs where the controlled parameters are the tendon stiffness values with a particular resolution.

Accurate and slow limb movements are quasi-static in the sense that the limb reaches a new state of equilibrium instantaneously in response to the control input. Here, the limb is neither in a state of *fixed equilibrium* under constant tendon forces, nor in a dynamic state with time-dependent tendon forces resisted by inertial accelerations of the limb. Inertial accelerations are negligible for slowly actuated, quasi-static, limb motions. These slow motions belong to a class of mechanical systems, known as *driftless*, where motion stops when actuation stops. Driftless systems arise in many applications, including satellite dynamics (Teel et al. 1995; Boscaïn and Chitour 2002), robotic vehicles (De Luca et al. 1998) and terrestrial and underwater biolocomotion (Shapere and Wilczek 1989; Kanso et al. 2005; Kanso 2009; Jing and Alben 2013). We apply these principles to examine the neuromechanical properties of *quasi-static* limb movements. A multi-muscle, multi-articular tendon-driven system has an actuation space (tendon stiffness parameters) with a dimension that is larger than the number of kinematic degrees of freedom. This is in contrast to most studies on driftless systems that consider underactuated motions, i.e., fewer actuation parameters than kinematic degrees of freedom (Kanso et al. 2005; Jing and Alben 2013). It is also unlike most robotics-type systems that have strictly 2 opposing tendons per kinematic degree of freedom (Inouye et al. 2012), or analyses that study limb function using rigid body dynamics driven by torques applied directly at the joints (Hogan 1985; Valero-Cuevas 2015). In tendon-driven limb movement, the forward problem of controlling the stiffness parameters that produce a desired slow limb movement is non-trivial because the solution is not unique. The rotation of each limb joint does not uniquely determine the lengths of all tendons crossing it (Valero-Cuevas 2015).

In this paper, we formulate the problem of accurate and slow movements in tendon-driven limbs as an overactuated (i.e., underdetermined) driftless system, controlled by changing the tendons' stiffness parameters. We follow the tradition of simple models that address the fundamental physics of biological function (see, for example, Srinivasan and Ruina 2006; Inouye and Valero-Cuevas 2016). Our mathematical approach is reminiscent to the rate control method proposed by Whitney 1969. It is also related to the control of limb impedance, another mathematical formulation well known in robotics (Hogan 1985). Here, we focus, from a physics and mechanics perspective, on the range of possible functions given the minimal assumption that muscle stiffness can be changed. We demonstrate that the control of stiffness suffices to produce stable and accurate limb postures and quasi-static transitions among them. This is in agreement

with the results from impedance control. However, we go beyond these results to offer a proof that stable postures are achievable only when tendons are pretensioned.

Altering tendon stiffness to produce equilibrium limb postures does not admit a unique solution due to the overactuated nature of the tendon-driven system; thus, the same posture can be achieved with multiple combinations of stiffness parameter values. Each combination places the system at a distinct strain energy level. Thus a same posture may be realized with different levels of strain energy. Therefore, we formulate the problem of stiffness control as an optimization problem (Ivaldi et al. 1988; Mussa-Ivaldi and Hogan 1991) that minimizes the strain energy of the limb. Further, we find that, for constant joint moment arms and tendon pretensioning values, optimal stiffness values depend on the change in the joint angle but not on the reference posture. This symmetry with respect to reference postures is broken in the case of posture-dependent moment arms.

Finally, we investigate the smoothness of quasi-static transitions among limb postures when the precision with which the stiffness is controlled is not infinitely smooth, that is to say, when the stiffness parameters are constrained to vary by small but finite increments. Under such constraints on precision, we observe discontinuities in the limb's quasi-static trajectories, indicating the existence of nearby unreachable postures because of insufficient stiffness precision. We also find that the precision with which stiffness needs to be controlled depends non-uniformly on the location in the limb's workspace.

## 2 Methods

We examine the slow movements of tendon-driven limbs in the context of a planar model system of an idealized finger model, see Fig. 1. The extensor mechanism of fingers is rather complex (Valero-Cuevas et al. 2007). Figure 1b shows a simplified setup of multi-articular muscles. To emphasize the generality of the mathematical framework, we consider the general case of a planar limb of  $n$  joints and let  $l_1, \dots, l_n$  be the lengths of the individual limb segments. The limb posture is defined by the column vector of joint angles  $\theta = (\theta_1, \dots, \theta_n)^T$  where the superscript  $()^T$  denotes the transpose operator. The joints are driven by  $m$  tendons ( $m > n$ ) of variable stiffness parameters  $k_i, i = 1, \dots, m$ , whose tendon paths produce an  $n \times m$  moment arm matrix  $\mathbf{R}(\theta)$ , see, e.g., Valero-Cuevas (2009), Valero-Cuevas (2015),

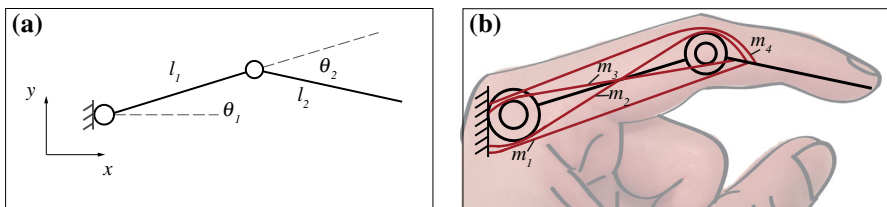


**Fig. 1** Finger model: kinematics (a) and muscle routing (b) overlaid on *top* of the physiological system

$$\mathbf{R} = \begin{pmatrix} r_{11} & r_{12} & \cdots & r_{1m} \\ \vdots & \vdots & \ddots & \vdots \\ r_{n1} & r_{n2} & \cdots & r_{nm} \end{pmatrix}. \tag{1}$$

Each entry  $r_{ij}$  (here,  $i = 1, \dots, c, n, j = 1, \dots, c, m$ ) denotes the “rotation” the  $j$ th tendon produces at the  $i$ th joint. It is positive when pulling the  $j$ th tendon induces a positive rotation (i.e., counterclockwise rotation per the right-hand rule).

We examine two types of joints: simple hinge joints where the moment arm matrix  $\mathbf{R}$  is constant for all values of  $\theta$ , and non-circular joints where the moment arm matrix is posture-dependent. In the finger model, the constant moment arm matrix is chosen to be

$$\mathbf{R} = \begin{pmatrix} -0.8 & -0.8 & 0.7 & 0.7 \\ -0.5 & 0.2 & -0.5 & 0.2 \end{pmatrix}, \tag{2}$$

in length units of cm. These values lie in the range of average moment arm values for the index finger reported in An et al. (1983) and Valero-Cuevas et al. (1998). For the posture-dependent moment arms, we define joint ellipses with semimajor and semiminor axes in the range of measured index moment arms found in An et al. (1983).

A change in limb posture corresponds to a rotation  $\Delta\theta = \theta_1 - \theta_o$  of the joints from a reference limb posture  $\theta_o$  to a new limb posture  $\theta_1$ . A rotation  $\Delta\theta$  fully determines the length changes  $\Delta\mathbf{s} = (\Delta s_1, \dots, \Delta s_m)^T$  of all tendons from their reference length. The length changes of the tendons are defined—without loss of generality—at the reference posture of the limb (An et al. 1983; Valero-Cuevas 2015),

$$\Delta\mathbf{s} = - \int_{\theta_o}^{\theta_1} (\mathbf{R}(\theta))^T d\theta = -\mathbf{R}^T \Delta\theta, \tag{3}$$

where the negative sign indicates that a positive rotation of the joint will shorten the tendons that induce it and vice versa.

For constant moment arms, the second equality in (3) is evident. In the case of posture-dependent moment arms, because we only consider small posture changes  $\Delta\theta$ , we use the trapezoid integration rule such that Eq. (3) holds with  $\mathbf{R} = (\mathbf{R}(\theta_o) + \mathbf{R}(\theta_1))/2$ , where  $\mathbf{R}(\theta_o)$  and  $\mathbf{R}(\theta_1)$  are the moment arm matrices evaluated at postures  $\theta_o$  and  $\theta_1$ , respectively.

We assume that each tendon is elastic and acts as a linear spring whose stiffness parameter is controlled to produce movement. We also allow each tendon to be pre-stretched from its resting length by an amount  $\Delta\mathbf{l}_o = (\Delta l_1, \dots, \Delta l_m)^T$ . Basically, each tendon has a baseline tension even at its reference length and does not go slack at any posture.

The total strain energy of the system,  $E$ , in the presence of tendon length changes  $\Delta\mathbf{s}$ , is then given by

$$E = \frac{1}{2} (\Delta\mathbf{s} + \Delta\mathbf{l}_o)^T \mathbf{K} (\Delta\mathbf{s} + \Delta\mathbf{l}_o). \tag{4}$$

As per the impedance (stiffness) control formulation (Hogan 1984), the stiffness matrix  $\mathbf{K}$  is an  $m \times m$  diagonal matrix of entries  $k_i$  corresponding to the stiffness of each muscle  $i$ .

$$\mathbf{K} = \begin{pmatrix} k_1 & \dots & 0 \\ \vdots & \ddots & \vdots \\ 0 & \dots & k_m \end{pmatrix}. \tag{5}$$

The associated muscle/tendon forces  $\mathbf{f} = (f_1, \dots, f_m)^T$  are given by

$$\mathbf{f} = -\mathbf{K}(\Delta\mathbf{s} + \Delta\mathbf{l}_0). \tag{6}$$

These tendon forces, in turn, produce torques  $\boldsymbol{\tau} = (\tau_1, \dots, \tau_n)^T$  at the joints defined by  $\boldsymbol{\tau} = \mathbf{R}\mathbf{f}$ .

A stable posture is achieved by satisfying the static equilibrium condition at the joints; namely, the total torque at each joint must be zero,

$$\boldsymbol{\tau} + \boldsymbol{\phi}(\boldsymbol{\theta}) = \mathbf{0}, \tag{7}$$

where  $\boldsymbol{\phi}(\boldsymbol{\theta}) = (\phi_1, \dots, \phi_n)^T$  denotes externally applied torques, such as gravity-induced torques at the joints of larger limbs. Slow, i.e., quasi-static, limb movements are achieved by sequentially satisfying this static equilibrium at each posture. It should be noted that the equilibrium condition means that the strain energy  $E$  is at a local minimum. That is to say, Eq. (7) is equivalent to being at a local minimum of the strain energy paraboloid described by Eq. (4). However, a posture can be at equilibrium at different energy levels. One has, at each posture, an admissible family of strain energy paraboloids, achievable at different combinations of spring stiffness  $K$  and excursion lengths  $\Delta\mathbf{s}$ . Figure 2 illustrates this concept schematically.

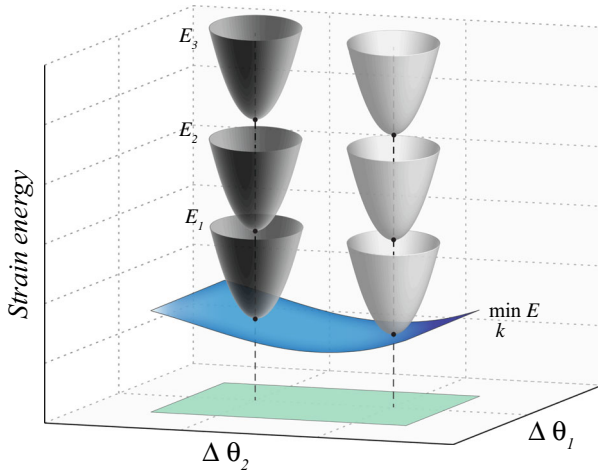


**Fig. 2** A sketch of the static equilibrium and energy optimization problem: For each sample posture, the static equilibrium condition can be satisfied at various combinations of stiffness values, corresponding to the minimum of each of many energy paraboloids. The optimization problem is solved by choosing the stiffness combination that minimizes the strain energy. The green plane is an example of the set of possible postures, and the blue surface represents a schematic illustration of the minimum strain energy manifold over this range of postures (Color figure online)

In the absence of external loading (for  $\phi = 0$ ), and if the tendons are not pretensioned ( $\Delta \mathbf{l}_0 = 0$ ), substituting (3) and (6) into  $\mathbf{Rf} = \mathbf{0}$  gives

$$\mathbf{RKR}^T \Delta \theta = 0, \tag{8}$$

which only admits the trivial solution  $\Delta \theta = 0$  for all  $\mathbf{K}$  because the  $n \times n$  square matrix  $\mathbf{RKR}^T$  is full rank when  $\mathbf{R}$  is full row rank. Thus, there exists only one trivial solution at the reference posture, and other stable postures are not achievable by varying  $\mathbf{K}$ . In contrast, when the tendons are pretensioned, one has

$$-\mathbf{RK}(-\mathbf{R}^T \Delta \theta + \Delta \mathbf{l}_0) = 0. \tag{9}$$

The system is thus unconditionally controllable, and equilibrium postures are achievable by proper choice of stiffness  $\mathbf{K}$ .

More generally, when the limb is subject to external load [nonzero  $\phi(\theta)$ ], the equilibrium condition (7) takes the form  $\mathbf{RKR}^T(\Delta \theta + \Delta \mathbf{l}_0) + \phi(\theta) = 0$ . Here, in the absence of muscle pretensioning ( $\Delta \mathbf{l}_0 = 0$ ), for each posture, i.e., for each value of  $\theta$ , one has one and only one solution  $\Delta \theta$  where the internal tendon-driven torques equal the external torques. This same posture can be achieved at various levels of muscle co-contraction, i.e., various values of  $\mathbf{K}$ , satisfying the equilibrium condition. However, posture controllability is limited to the solution of this equality. In contrast, when the tendons are pretensioned ( $\Delta \mathbf{l}_0 \neq 0$ ), the system is again unconditionally controllable by proper choice of stiffness parameters  $\mathbf{K}$ . Since the external load  $\phi(\theta)$  does not qualitatively affect the system controllability, we hereafter set  $\phi$  to zero to model a limb with no external load and low inertia such as a finger.

It should be noted here that our work relates to the situation where muscle stiffness is arbitrarily controlled, where even if a joint rotation lengthens a muscle, the nervous system can command that muscle to reduce or increase its stiffness. Mathematically speaking, for a given reference posture and pretensioning level  $\Delta \mathbf{l}_0$ , there exist several combinations of stiffness  $\mathbf{K}$  that satisfy the static equilibrium condition. We choose the pretensioning values  $\Delta \mathbf{l}_0$  to ensure that the tendons are nowhere slack in the workspace. Thus, equilibrium postures  $\theta$  can be computed without imposing additional restrictions on  $\Delta \mathbf{l}_0$ .

Our quasi-static formulation implies that, starting from a given initial posture, the limb has to transition to “nearby” equilibrium postures, that is to say,  $\Delta \theta$  must be small. A large value of  $\Delta \theta$  means that the limb would instantaneously jump from its current posture to a far away equilibrium posture, which violates the slow movement assumption. Therefore, in all subsequent analyses, we consider quasi-static transitions to only nearby postures. In particular, we formulate: (1) an *optimality problem* where for a given equilibrium posture  $\theta$ , we solve for optimal stiffness values that minimize the strain energy function associated with transitions to nearby postures, and (2) a *reachability problem* where we explore reachable equilibrium postures for given stiffness values.

### 2.1 Optimal Equilibrium Postures

Starting at a posture  $\theta_o$ , a desired limb posture  $\theta$  near  $\theta_o$  can be achieved by tuning the tendon stiffness parameters so that the vector  $(-\mathbf{R}^T \Delta\theta + \Delta\mathbf{l}_o)$  in Eq. (9) lies in the null space of the  $n \times m$  matrix  $\mathbf{RK}$ . The resulting stiffness values are not unique, in general. For each limb posture  $\theta$ , Eq. (9) yields a family of solutions  $\mathbf{K}$ , at multiple strain energy levels, for which  $\theta$  is achievable (Fig. 2). This redundancy leads us to look for optimal stiffness values  $\mathbf{K}_{opt}$  that minimize the strain energy function while satisfying the equilibrium constraint and inequality constraints on permissible stiffness values, namely,

$$\begin{aligned} \min_{\mathbf{K}} \left[ E = \frac{1}{2}(-\mathbf{R}^T \Delta\theta + \Delta\mathbf{l}_o)^T \mathbf{K}(-\mathbf{R}^T \Delta\theta + \Delta\mathbf{l}_o) \right] \\ \text{subject to } -\mathbf{RK} \left( -\mathbf{R}^T \Delta\theta + \Delta\mathbf{l}_o \right) + \phi(\theta) = 0, \tag{10} \\ \text{and } k_{\min} \leq k_i \leq k_{\max}, \\ k_{\min} > 0. \end{aligned}$$

where we set  $\phi(\theta) = 0$  in the finger model and define practical limits on the values of the stiffnesses  $k_i$ . This optimization problem is linear in the sense that the strain energy (cost) function and the constraints are all linear in  $\mathbf{K}$ . This suggests the possibility of degenerate minima if either the strain energy or constraints functions are linearly dependent. We posit that this is an unlikely design in biological and man-made systems; the numerical results presented in this study are not degenerate.

### 2.2 Reachable Equilibrium Postures

Given a specific combination of stiffness parameters  $\mathbf{K}$ , the achievable equilibrium posture  $\theta$  can be found by solving the “forward problem” in (9), which we rewrite as  $\mathbf{RKR}^T \Delta\theta = \mathbf{RK}\Delta\mathbf{l}_o$ . That is, given an initial posture  $\theta_o$  and muscle stiffness  $\mathbf{K}$ , we compute a new posture  $\theta = \theta_o + \Delta\theta$  that satisfies the equilibrium condition (7). Given that the matrix  $\mathbf{RKR}^T$  is invertible, solutions to this forward problem are unique: For each  $\mathbf{K}$ , there exists one and only one  $\Delta\theta$ , which in turn gives a uniquely defined new equilibrium posture  $\theta$ . While the new posture  $\theta$  is at equilibrium in the sense that it corresponds to a local minimum of the strain energy paraboloid  $E$ , it does not necessarily correspond to the minimum of all possible energy levels. That is to say, no particular effort is made here to ensure optimality of the equilibrium postures. But as in the optimality problem, we only examine small changes of equilibrium posture  $\Delta\theta$ . We systematically sample the stiffness space at different precision levels, i.e., degrees of discretization granularity  $\Delta k$ . For each precision level  $\Delta k$ , we calculate the set of admissible departures  $\Delta\theta$  from a reference posture and consequently the set of reachable (feasible) postures  $\theta$ . The goal here is not to minimize the strain energy at each reachable posture because the forward problem (computing  $\Delta\theta$  given  $\mathbf{K}$ ) admits a unique solution. Rather, our goal is to find the set of all nearby reachable postures as a function of the precision with which individual stiffnesses can be controlled.

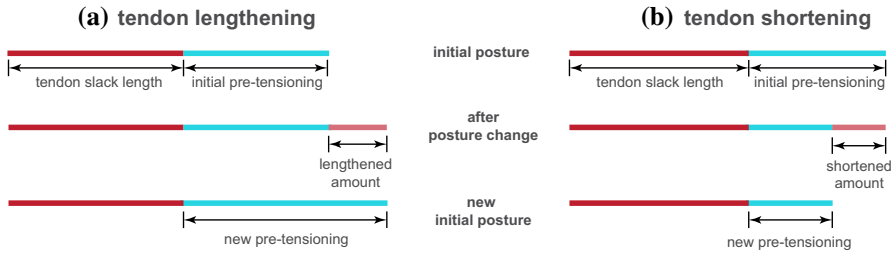


**Fig. 3** Variable pretensioning update rule: The pretensioning is history-dependent, taking into account the tendon’s lengthening (a) or shortening (b) that took place in the previous posture change

### 2.3 Parameter Values

A few remarks on the parameter values of  $k_{\min}$  and  $k_{\max}$  are in order here.  $k_{\min}$  is always greater than zero ensuring that the optimization problem is well posed. Here, we choose a range of stiffness values  $k_{\min} = 100$  to  $k_{\max} = 1000$  N/m, in agreement with experimental data that measured stiffness in a variety of muscles ranging from those that actuate a finger to those of a leg (Rätsep and Asser 2011; Chuang et al. 2012; Bizzini and Mannion 2003; Mustalampi et al. 2013). We now non-dimensionalize all parameters using a characteristic length scale  $l^* = 10$  cm and a characteristic force  $f^* = 100$  N. Non-dimensional parameters enable us to obtain generic results, which we can later easily scale up or scale down to different limb sizes. Using the characteristic length and force scales, the dimensionless range of stiffness values is  $k_{\min} = 0.1$  to  $k_{\max} = 1$ —making  $\Delta k = 0.05$  equal to 5% of the range. The normalized values of the pre-stretched lengths  $\Delta l_i$  are all set to 0.1 in the finger model. Note that in addition to constant pre-stretch, we consider pre-stretched lengths that vary with posture.

### 2.4 Pretensioning of the Tendons

We investigate the effect of constant versus variable tendon pretensioning. Constant pretensioning means that the system is “memoryless” and resets to the initial  $\Delta l_o$  because pretensioning does not depend on the previous tendon lengths. Variable pretensioning is defined according to the update rule depicted in Fig. 3, where the pretensioning value at each posture is equal to that at the previous posture plus the cumulative change in tendon length that occurred as a result of moving from the previous to the current posture; thus, the pretensioning has “memory.”

### 2.5 Workspace of the Finger Endpoint

We now focus on the finger model presented in Fig. 1. Given  $\theta = (\theta_1, \theta_2)^T$ , the finger’s posture in the  $(x, y)$ -plane follows in a straightforward way

$$x_w = l_1 \cos \theta_1 + l_2 \cos(\theta_2 - \theta_1), \quad y_w = l_1 \sin \theta_1 + l_2 \sin(\theta_2 - \theta_1). \quad (11)$$

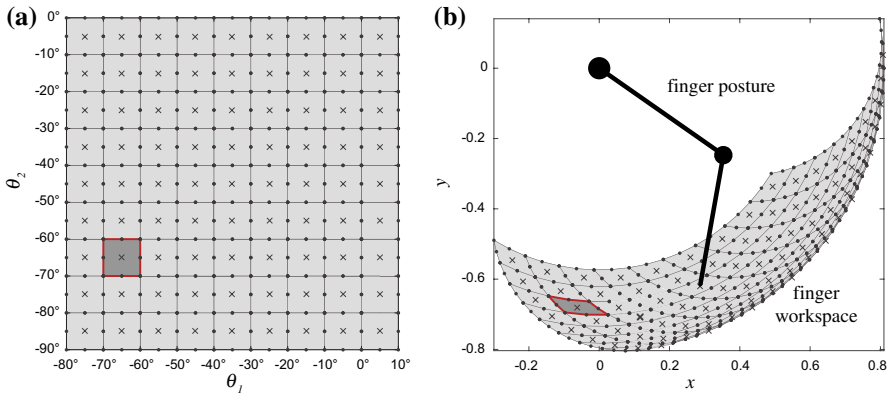


**Fig. 4** Finger model: **a** configuration space and **b** the corresponding endpoint space which deforms the squares into “diamonds”

The finger workspace  $W$  is the set of all points  $(x_w, y_w)$  of the  $(x, y)$ -plane accessible by the finger’s endpoint for all admissible  $\theta_1$  and  $\theta_2$ . A depiction of the joint angles space and the workspace of the finger model is shown in Fig. 4. Here, the admissible joint angles are taken to lie in the range  $\theta_1 \in [-80^\circ, 10^\circ]$ ,  $\theta_2 \in [0^\circ, 90^\circ]$ . Initial postures  $\theta_o$  in this admissible range are discretized using a  $9 \times 9$  regular grid, marked by  $\times$ . For each  $\theta_o$ , we explore optimal transitions to equilibrium postures in a small square neighborhood centered at  $\theta_o$  and of side length  $10^\circ$ . More specifically, we consider a total of nine nearby equilibrium postures, including staying at the initial posture  $\theta_o$ . We compute the optimal stiffness values for the change in joint angles  $\Delta\theta$  associated with a transition from the initial posture to each of these nine postures. We linearly interpolate these values in the neighborhood of each initial posture to construct a complete map of optimal stiffness values.

### 2.6 Quasi-Static Trajectories of the Finger

We consider quasi-static trajectories where the finger endpoint is required to slowly trace, back and forth, curved and straight lines in the workspace as depicted in Fig. 5. We solve for the optimal stiffness combinations required by the limb to perform this back and forth motion. To this end, the quasi-static trajectories are discretized, and the optimization problem in Eq. (10) is solved sequentially along the discrete trajectory.

### 2.7 Reachable Sets in the Finger Workspace

We discretize the range of stiffness values from  $k_{\min}$  to  $k_{\max}$  using constant increments  $\Delta k$ , producing  $M = (k_{\max} - k_{\min})/\Delta k + 1$  discrete stiffness values for each tendon. For  $m$  tendons, this discretization generates  $M^m$  different stiffness matrices  $\mathbf{K}$ , which amounts essentially to a uniform sampling of the  $m$ -dimensional stiffness space. For example, setting  $\Delta k = 0.05$  in the finger model amounts to  $19^4$  distinct  $\mathbf{K}$  matrices.

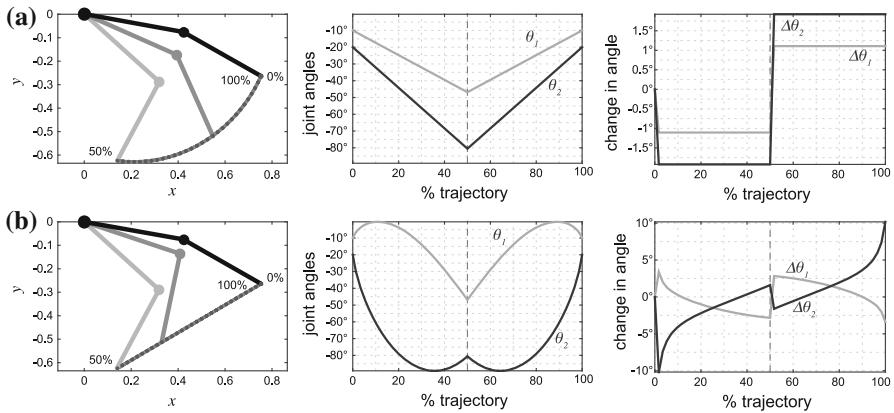


**Fig. 5** Endpoint trajectories for the finger model: Finger endpoint is required to trace **a** a curved trajectory, **b** a straight line. Subfigures depict the prescribed values of  $(x_w, y_w)$  and associated  $(\theta_1, \theta_2)$  and  $(\Delta\theta_1, \Delta\theta_2)$

For each  $\mathbf{K}$ , we solve Eq. (9) to compute  $\Delta\theta$  starting from a reference posture  $\theta_o$  and use (11) to compute the reachable endpoint location  $(x_w, y_w)$ . We constrain the full set of  $M^m$  reachable points to those that are in the vicinity of the reference posture.

### 3 Results

#### 3.1 Quasi-Static Trajectories

Figure 6 depicts the optimal stiffness values for the finger model tracing the trajectories of Fig. 5a, b for all combinations of moment arms and pretensioning scenarios. The optimal stiffness values are characterized by a local jump as the limb reverses its motion to trace the trajectory backward. The jump in the stiffness of certain tendons gets attenuated in the case of variable moment arms, but all jumps get smoothed out completely when the pretensioning is changing continuously with posture. In these cases, one observes the relaxation of the some tendons during the activity of the opposing tendons, and the opposite effect is clearly seen during the return portion of the movement.

#### 3.2 Optimal Equilibrium Postures over the Whole Workspace

Figure 7 depicts the optimal stiffness values  $\mathbf{K}_{opt}$  for the finger model with constant moment arms  $\mathbf{R}$  and constant pretensioning  $\Delta\mathbf{l}_o$  over the whole workspace. Note that the workspace is discretized as depicted in Fig. 4 and described in the previous section. Tendons  $m_2$  and  $m_4$  exhibit higher stiffness values than  $m_1$  or  $m_3$ . A closer look at the stiffness variation within each neighborhood shows that, in the context of constant moment arms, all neighborhoods are identical, that is to say, optimal stiffness values depend only on the change in joint angles  $\Delta\theta$ , or posture change, and not on the initial

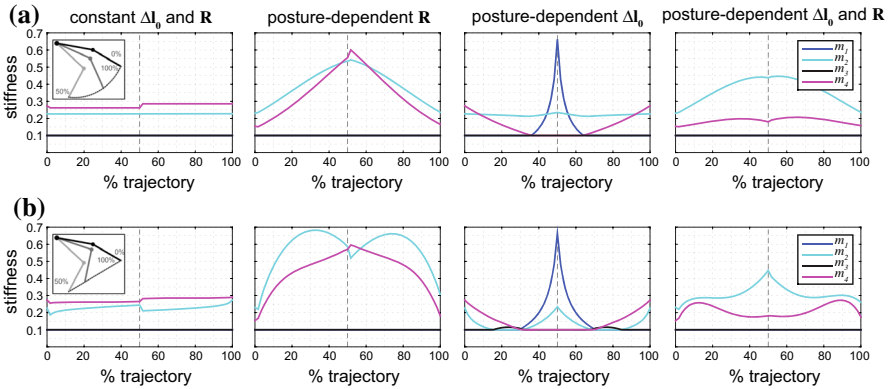


**Fig. 6** Finger model: optimal stiffness values for the quasi-static trajectories shown in Fig. 5a, b. Please note that, for quasi-static movements lasting multiple seconds, the delay in excitation–contraction dynamics (c. 35 ms) should not be a limiting factor to the need for large changes in muscle stiffness

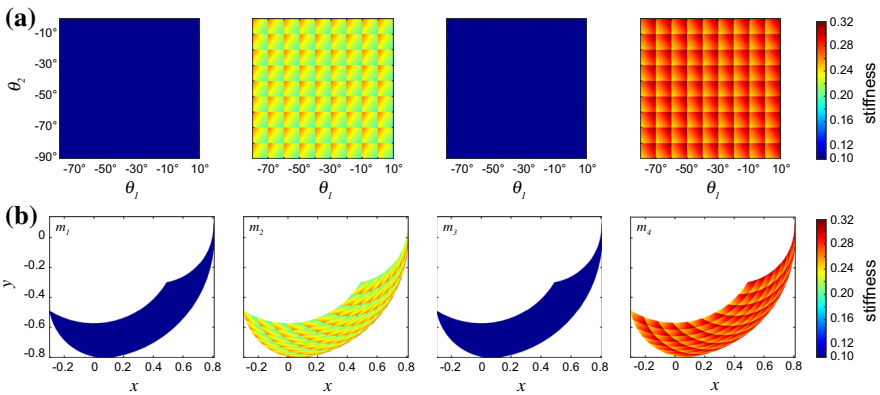


**Fig. 7** Finger model with constant moment arms: optimal stiffness parameters needed to achieve each posture in **a** configuration (*joint angle*) space and **b** endpoint space. The *plots* show the stiffness levels of each tendon  $m_i$ ,  $i = 1, \dots, 4$ , that minimize the strain energy function

posture. Further, the stiffness variation within each neighborhood is such that  $m_2$  and  $m_4$  counterbalance each other in the  $\theta_1$ -direction—as the stiffness of  $m_2$  increases, that of  $m_4$  decreases and vice versa.

Figure 8 depicts the optimal stiffness values for the case when the moment arms vary with joint angles. As in the case of constant moment arms,  $m_2$  and  $m_4$  require higher stiffness values, and the neighborhood around each initial posture indicates that each tendon has a “preferred” direction of higher stiffness, which is the same as in Fig. 7. However, the optimal stiffness values now depend on moment arms and thus on initial posture. Interestingly, the stiffness variation across the whole workspace is also characterized by  $m_2$  and  $m_4$  counterbalancing each other, indicating an obligatory covariation in the way this pair of muscles acts in transitions to nearby equilibrium postures and to postures across the whole workspace.

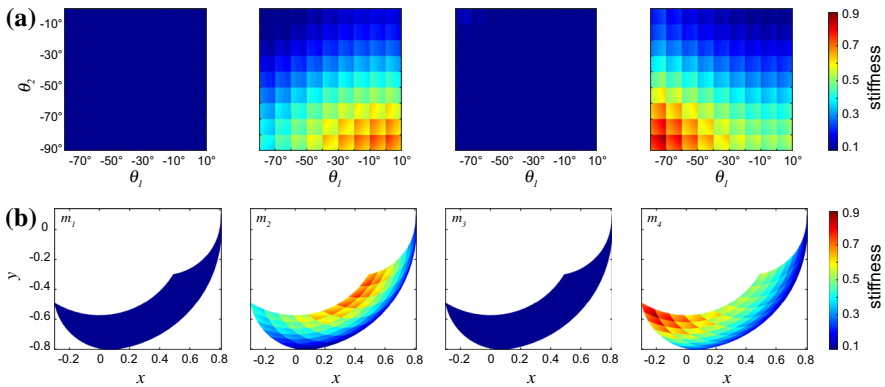


**Fig. 8** Finger model with posture-dependent moment arms

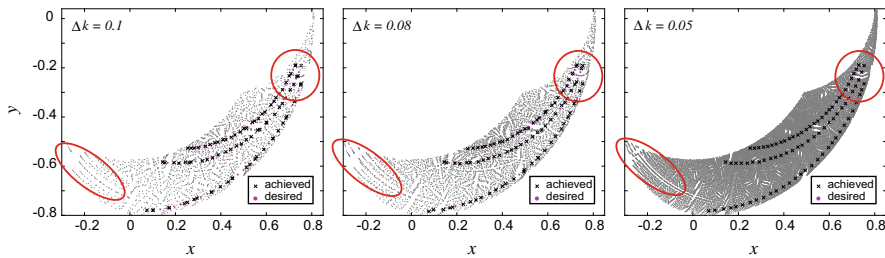


**Fig. 9** Finger model: achievable versus desired trajectories overlaid on *top* of the reachable postures. The level of stiffness precision affects the reachability. As precision increases (from *left to right*), the endpoint trajectories become smoother and closer to the desired trajectories. Discontinuities in the set of reachable points vary nonlinearly in the workspace, e.g., regions highlighted in *red* (Color figure online)

### 3.3 Reachable Equilibrium Postures

We explore the reachability or feasibility of tracing certain trajectories within the limb’s workspace given constraints on the precision in the control of stiffness. For illustration purposes, we investigate the ability of the finger model to trace multiple trajectories for a given  $\Delta k$ . Starting from the initial posture, we sequentially transition to the next point along the trajectory by locating the nearest admissible reachable posture. Figure 9 shows the desired versus reachable endpoint trajectories for three precision levels  $\Delta k = 0.1, 0.08, 0.05$ , superimposed on the set of all reachable points in the limb workspace. The reachable paths show discontinuities. These discontinuities decrease as the resolution of stiffness increases, going from  $\Delta k = 0.1$  and  $\Delta k = 0.05$ , and eventually disappear as  $k$  is varied continuously. The discontinuous behavior arises from unreachable nearby desired postures along the discretized path, in which case the limb settles at the nearest admissible posture from the set of reachable nearby postures. Further, we observe that discontinuities exhibit a nonlinear structure in the limb workspace, implying that the demands on the precision in stiffness vary nonlinearly in space.

## 4 Discussion

We developed a novel mathematical formulation for slow and accurate tendon-driven limb movements using the framework of *driftless* mechanical systems where movement is generated by controlling the tendons' stiffness parameters. We used this framework to address three questions in slow limb movements: (1) Can slow limb movements be achieved by modulating the stiffness parameters only? (2) what is the role of pretensioning? and (3) how are these movements affected by limits on the precision with which stiffness can be controlled? We demonstrated that stiffness control is sufficient to produce accurate and slow limb movements, but only when the tendons are pre-stretched. We then probed the limb's ability to trace prescribed trajectories. When the moment arm  $\mathbf{R}$  or muscle pretensioning  $\Delta \mathbf{l}_o$  are held constant, the stiffness values required to track the prescribed trajectories are characterized by sharp "kinks" or discontinuities, which get smoothed out for posture-dependent  $\mathbf{R}$  and  $\Delta \mathbf{l}_o$ .

We analyzed the reachability of the limb's workspace by exploring the limb's ability to trace prescribed trajectories under constraints on stiffness precision. Here, we did not impose any restriction on the strain energy level. By comparing different levels of precision (i.e., resolution) to control stiffness, we found that high resolution of stiffness is key for the limb to improve its accuracy in tracking a trajectory. More specifically, we identified discontinuous patterns in the limb workspace at low muscle precision that almost disappeared at higher precision. Our results also revealed that the required stiffness resolution is not uniform throughout the limb's workspace in the sense that lower muscle resolutions induce discontinuities that are non-uniform and are localized to certain regions of the workspace.

In addition to their direct relevance to understanding the necessary conditions and limitations of bio-inspired, tendon-driven robotic limbs, our results bear relevance to the neural control of movement. In that literature, slow limb movements are, to our knowledge, not addressed. Limb movements in general have at times been considered from the perspectives of impedance control, force-field primitives, spinal feedback systems (Giszter et al. 2007; Giszter 2015), or the framework of the *equilibrium point hypothesis* (EPH), which states that limb movements are generated by a sequence of equilibrium points along a desired trajectory (Asatryan and Feldman 1965; Feldman and Levin 2009; Cooke 1980). Our mathematical formulation is reminiscent of but not identical to these approaches. EPH, for example, considers that the magnitude of the "control" force exerted on the limb, at any time, depends on the difference between the "actual" limb dynamics and the desired equilibrium point, and derives a second-order differential equation for the "error" between the actual and desired dynamics (Shadmehr 1998; Asatryan and Feldman 1965; Feldman 1966). Here, we were not concerned with the relaxation dynamics. Our working hypothesis is that this relaxation timescale is much faster than the timescale associated with slow limb movements, and the limb reaches a state of equilibrium instantaneously in response to changes in muscle stiffness. Our formulation focused on determining whether equilibrium postures of multi-joint limbs and quasi-static transitions among them can be achieved by direct control of muscle stiffness values and the effect of stiffness resolution on achievable postures.

The direct control of muscle stiffnesses can be viewed as an abstraction, or “meta-model,” of muscle control. While the fact that muscles have stiffness (and strain energy)—and that the nervous system can regulate them—is well established (e.g., [Mussa-Ivaldi and Hogan 1991](#); [Burdet et al. 2000, 2001](#)), our main goal was to present a general mathematical framework for analyzing slow limb movements that arise from the control of muscle stiffness, rather than to focus on the details of the production and control of muscle stiffness. In addition, our use of high- and low-resolution regulation of stiffness is not meant to indicate a discontinuity in the time history of the neural control signal. Rather, it is simply a means to indicate a lack of accuracy in the production of a given level of muscle stiffness at a given posture. Signal-dependent noise and motor unit recruitment and rate coding are well-known sources of such inaccuracies and high-frequency variability.

Experimental work on muscle force has shown that if a muscle is clamped at a constant length and stimulated (an isometric contraction), its active force depends on the length in a non-monotonic way, with lower force at short or long lengths and a maximum force at some length in between. This effect is called the force–length relationship. Importantly, the force–length relationship is not like a Hook’s law for muscle (i.e., a stress vs. strain relationship). It simply represents the amount of active isometric contractile force a muscle can produce at a given length but not directly its passive stiffness. In addition, if a muscle is allowed to shorten (a concentric contraction), the force will also depend on the shortening speed, decreasing as the shortening speed gets higher. If the muscle is lengthened by some external force, even as it produces force to resist the lengthening (an eccentric contraction), the active force increases above the isometric value ([McMahon 1984](#); [Chen et al. 2011](#)). Together, these effects are called the force–velocity relationship and can be modeled succinctly as done in [Hill \(1938\)](#) and [Williams \(2010\)](#) using a mathematical product of these two effects and an activation function. Given that our study is concerned with slow limb movements, one can reasonably argue that the shortening velocity is slow and can be considered a constant. An interesting outcome of our formulation is that, although we use a spring model for the muscles, the muscle forces required to trace a trajectory are not necessarily linear. Indeed, a re-drawing of the muscle stiffnesses  $k_i$  reported in [Fig. 6](#) as functions of the joint angles and thus of muscle lengths would reveal a highly nonlinear dependence of  $k_i$  on the change in muscle length  $\Delta s_i$ . A detailed analysis of this non-linearity, as well as how to incorporate the Hill-type force model into our formulation, will be the topic of future work.

Another future direction is to investigate the similarities between the discontinuities observed in [Fig. 9](#) and the discontinuous nature of slow finger movements reported in numerous experimental studies ([Vallbo and Wessberg 1993](#); [Darling et al. 1994](#)). Several studies attributed these discontinuities to neural sources, while others held responsible peripheral stretch reflexes ([Gross et al. 2002](#); [Williams et al. 2009](#); [Evans and Baker 2003](#)). Our formulation offers a novel framework that can be used in conjunction with further experimentation to decipher the origins of these discontinuities and their dependence on the nature and integrity of the neural control of musculature in health and disease.

Most importantly, this work serves to define the neuromechanical boundary conditions that make slow movements possible and effective. We establish the physical

nature of slow limb movements in the context of changes in strain energy, regardless of the physiological mechanisms that bring this about. Our two main results, in particular, serve to direct future research. First, we establish that pretensioning of muscles is necessary to produce slow movements. Second, there are real mechanical consequences to the quality of the movement that depend directly on the resolution with which muscle stiffness (or strain energy) is controlled. Together these results may begin to explain the evolutionary pressures that drove the development of the spinal circuitry and mechanisms needed for regulating muscle tone in vertebrates and for the orderly recruitment and rate coding of muscle fibers.

**Acknowledgments** S. B. and F. V. C. were partially supported by the grants NIH R01AR050520, NIH R01AR052345, NIDRR H133E080024 and NSF EFRI-COPN 0836042, and S. B. and E. K. by the Grants NSF CMMI-0644925 and NSF CCF-0811480. The content is solely the responsibility of the authors and does not necessarily represent the official views of the National Institutes of Health.

**Conflict of interest** The authors declare that they have no conflict of interest.

## References

- An, K., Ueba, Y., Chao, E., Cooney, W., Linscheid, R.: Tendon excursion and moment arm of index finger muscles. *J. Biomech.* **16**(6), 419–425 (1983)
- Asatryan, D.G., Feldman, A.G.: Functional tuning of the nervous system with control of movement or maintenance of a steady posture: I. mechanographic analysis of the work of the joint or execution of a postural task. *Biophysics* **10**(5), 925–934 (1965)
- Bizzini, M., Mannion, A.F.: Reliability of a new, hand-held device for assessing skeletal muscle stiffness. *Clin. Biomech.* **18**(5), 459–461 (2003)
- Boscaiu, U., Chitour, Y.: On the minimum time problem for driftless left-invariant control systems on so (3). *Commun. Pure Appl. Anal.* **1**, 285–312 (2002)
- Burdet, E., Osu, R., Franklin, D., Yoshioka, T., Milner, T., Kawato, M.: A method for measuring endpoint stiffness during multi-joint arm movements. *J. Biomech.* **33**(12), 1705–1709 (2000)
- Burdet, E., Osu, R., Franklin, D.W., Milner, T.E., Kawato, M.: The central nervous system stabilizes unstable dynamics by learning optimal impedance. *Nature* **414**(6862), 446–449 (2001)
- Chen, J., Tian, J., Iwasaki, T., Friesen, W.O.: Mechanisms underlying rhythmic locomotion: dynamics of muscle activation. *J. Exp. Biol.* **214**(11), 1955–1964 (2011)
- Chuang, L.-L., Wu, C.-Y., Lin, K.-C.: Reliability, validity, and responsiveness of myotonometric measurement of muscle tone, elasticity, and stiffness in patients with stroke. *Arch. Phys. Med. Rehabil.* **93**(3), 532–540 (2012)
- Cooke, J.: The organization of simple, movements. In: Stelmach, G.E., Requin, J. (eds.) *Tutorials in Motor Behavior*, pp. 199–212. North Holland Publishing Company, Amsterdam (1980)
- Darling, W.G., Cole, K.J., Miller, G.F.: Coordination of index finger movements. *J. Biomech.* **27**(4), 479–491 (1994)
- De Luca, A., Oriolo, G., Samson, C.: *Feedback Control of a Nonholonomic Car-like Robot*, Book Section 4, pp. 171–253. Springer, New York (1998)
- Evans, C., Baker, S.N.: Task-dependent intermanual coupling of 8-hz discontinuities during slow finger movements. *Eur. J. Neurosci.* **18**(2), 453–456 (2003)
- Feldman, A.: Functional tuning of the nervous system with control of movement or maintenance of a steady posture. ii. controllable parameters of the muscle. *Biophysics* **11**(3), 565–578 (1966)
- Feldman, A.G., Levin, M.F.: *The Equilibrium-Point Hypothesis—Past, Present and Future*, vol. 629. Springer, Berlin (2009)
- Frecker, M., Snyder, A.J.: Surgical robotics: multifunctional end effectors for robotic surgery. *Oper. Techn. Gen. Surg.* **7**(4), 165–169 (2005)

- Giszter, S., Patil, V., Hart, C.: Primitives, premotor drives, and pattern generation: a combined computational and neuroethological perspective. *Prog. Brain Res.* **165**, 323–346 (2007)
- Giszter, S.F.: Motor primitives—new data and future questions. *Curr. Opin. Neurobiol.* **33**, 156–165 (2015)
- Gross, J., Timmermann, L., Kujala, J., Dirks, M., Schmitz, F., Salmelin, R., Schnitzler, A.: The neural basis of intermittent motor control in humans. *Proc. Natl. Acad. Sci.* **99**(4), 2299–2302 (2002)
- Hill, A.: The heat of shortening and the dynamic constants of muscle. *Proc. R. Soc. Lond. B Biol. Sci.* **126**(843), 136–195 (1938)
- Hogan, N.: Adaptive control of mechanical impedance by coactivation of antagonist muscles. *Autom. Control IEEE Trans.* **29**(8), 681–690 (1984)
- Hogan, N.: Impedance control: an approach to manipulation: Part II—implementation. *J. Dyn. Syst. Meas. control* **107**(1), 8–16 (1985)
- Inouye, J.M., Kutch, J.J., Valero-Cuevas, F.J.: A novel synthesis of computational approaches enables optimization of grasp quality of tendon-driven hands. *Robot. IEEE Trans.* **28**(4), 958–966 (2012)
- Inouye, J.M., Valero-Cuevas, F.J.: Muscle synergies heavily influence the neural control of arm endpoint stiffness and energy consumption. *PLoS Comput. Biol.* **12**(2), e1004737 (2016)
- Ivaldi, F.M., Morasso, P., Zaccaria, R.: Kinematic networks. *Biol. Cybern.* **60**(1), 1–16 (1988)
- Jing, F., Alben, S.: Optimization of two-and three-link snakelike locomotion. *Phys. Rev. E* **87**(2), 022711 (2013)
- Jung, S.-Y., Kang, S.-K., Lee, M.-J., Moon, I.: Design of robotic hand with tendon-driven three fingers. In: *Control, Automation and Systems, 2007. ICCAS'07. International Conference on, IEEE, Year*, pp. 83–86
- Kanso, E.: Swimming due to transverse shape deformations. *J. Fluid Mech.* **631**, 127–148 (2009)
- Kanso, E., Marsden, J.E., Rowley, C.W., Melli-Huber, J.: Locomotion of articulated bodies in a perfect fluid. *J. Nonlinear Sci.* **15**(4), 255–289 (2005)
- Lee, Y.-T., Choi, H.-R., Chung, W.-K., Youm, Y.: Stiffness control of a coupled tendon-driven robot hand. *Control Syst. IEEE* **14**(5), 10–19 (1994)
- McMahon, T.A.: *Muscles, Reflexes, and Locomotion*. Princeton University Press, Princeton (1984)
- Mussa-Ivaldi, F.A., Hogan, N.: Integrable solutions of kinematic redundancy via impedance control. *Int. J. Robot. Res.* **10**(5), 481–491 (1991)
- Mustalampi, S., Häkkinen, A., Kautiainen, H., Weir, A., Ylinen, J.: Responsiveness of muscle tone characteristics to progressive force production. *The J. Strength Cond. Res.* **27**(1), 159–165 (2013)
- Rätsep, T.O., Asser, T.: Changes in viscoelastic properties of skeletal muscles induced by subthalamic stimulation in patients with parkinson's disease. *Clin. Biomech.* **26**(2), 213–217 (2011)
- Shadmehr, R.: *The Equilibrium Point Hypothesis for Control of Movement*. Department of Biomedical Engineering, Johns Hopkins University, Baltimore (1998)
- Shapere, A., Wilczek, F.: Geometry of self-propulsion at low reynolds number. *J. Fluid Mech.* **198**, 557–585 (1989)
- Simaan, N., Xu, K., Wei, W., Kapoor, A., Kazanzides, P., Taylor, R., Flint, P.: Design and integration of a telerobotic system for minimally invasive surgery of the throat. *Int. J. Robot. Res.* **28**(9), 1134–1153 (2009)
- Srinivasan, M., Ruina, A.: Computer optimization of a minimal biped model discovers walking and running. *Nature* **439**(7072), 72–75 (2006)
- Teel, A.R., Murray, R.M., Walsh, G.C.: Non-holonomic control systems: from steering to stabilization with sinusoids. *Int. J. Control* **62**(4), 849–870 (1995)
- Valero-Cuevas, F.J.: A mathematical approach to the mechanical capabilities of limbs and fingers. In: Sternad, D. (ed.) *Progress in Motor Control. Advances in Experimental Medicine and Biology*, vol. 629, pp. 619–633. Springer (2009)
- Valero-Cuevas, F.J.: *Fundamentals of Neuromechanics*, vol. 8 of *Biosystems and Biorobotics*. Springer, London (2015)
- Valero-Cuevas, F.J., Yi, J.-W., Brown, D., McNamara, R.V., Paul, C., Lipson, H.: The tendon network of the fingers performs anatomical computation at a macroscopic scale. *Biomed. Eng. IEEE Trans.* **54**(6), 1161–1166 (2007)
- Valero-Cuevas, F.J., Zajac, F.E., Burgar, C.G.: Large index-fingertip forces are produced by subject-independent patterns of muscle excitation. *J. Biomech.* **31**(8), 693–703 (1998)
- Vallbo, A., Wessberg, J.: Organization of motor output in slow finger movements in man. *J. Phys.* **469**(1), 673–691 (1993)

- Whitney, D.E.: Resolved motion rate control of manipulators and human prostheses. *IEEE Trans. Man Machine*. **MMS-10**(2), 47–53 (1969). doi:[10.1109/TMMS.1969.299896](https://doi.org/10.1109/TMMS.1969.299896)
- Williams, E.R., Soteropoulos, D.S., Baker, S.N.: Coherence between motor cortical activity and peripheral discontinuities during slow finger movements. *J. Neurophysiol.* **102**(2), 1296–1309 (2009)
- Williams, T.L.: A new model for force generation by skeletal muscle, incorporating work-dependent deactivation. *J. Exp. Biol.* **213**(4), 643–650 (2010)